

## Structural and transport studies of $\text{CeRu}_{2-x}\text{Co}_x\text{Ge}_2$

This article has been downloaded from IOPscience. Please scroll down to see the full text article.

2005 J. Phys.: Condens. Matter 17 313

(<http://iopscience.iop.org/0953-8984/17/2/007>)

View [the table of contents for this issue](#), or go to the [journal homepage](#) for more

Download details:

IP Address: 129.252.86.83

The article was downloaded on 27/05/2010 at 19:44

Please note that [terms and conditions apply](#).

# Structural and transport studies of $\text{CeRu}_{2-x}\text{Co}_x\text{Ge}_2$

**R Rawat and V G Sathe**

UGC DAE Consortium for Scientific Research, University Campus, Khandwa Road,  
Indore-452017, MP, India

E-mail: rrawat@udc.ernet.in

Received 29 October 2004, in final form 22 November 2004

Published 20 December 2004

Online at [stacks.iop.org/JPhysCM/17/3/13](http://stacks.iop.org/JPhysCM/17/3/13)

## Abstract

The crystal structure and electric transport properties of the compounds  $\text{CeRu}_{2-x}\text{Co}_x\text{Ge}_2$  ( $x = 0.0\text{--}2.0$ ) have been investigated. The magnetic behaviour of this system is correlated with the structural parameters. Based on these studies, a magnetic phase diagram has been proposed for this system. A transition from a magnetic ground state to a non-magnetic ground state has been observed with increasing Co concentration. It is found that the Ce–Ru/Co bond distance plays a critical role in driving the system from an RKKY dominated regime to a Kondo regime.

## 1. Introduction

Ce-based ternary compounds  $\text{CeT}_2\text{X}_2$  ( $T =$  transition metals,  $X = \text{Si, Ge}$ ) with the  $\text{ThCr}_2\text{Si}_2$  type tetragonal structure exhibit a rich variety of ground states like the Kondo effect, different magnetic structures, non-Fermi liquid behaviour, etc [1]. In most of these compounds, the magnetic ground state is an interplay of two interactions: an RKKY (Ruderman–Kittel–Kasuya–Yosida) interaction and the Kondo effect. Both the interactions depend on the product of exchange interaction  $J$  (between the conduction electron and localized f-electrons) and  $N$  (density of state at the Fermi level). The strength of the RKKY interaction  $T_{\text{RKKY}}$  has  $(JN)^2$  dependence whereas the Kondo interaction strength  $T_{\text{K}}$  has  $\exp(-1/JN)$  dependence. The competition between these two interactions can be explained qualitatively using the one-dimensional Kondo necklace model [2]. In this model, for small  $JN$  ( $T_{\text{RKKY}} > T_{\text{K}}$ ), the RKKY interaction dominates and the system orders magnetically, whereas for large  $JN$  ( $T_{\text{RKKY}} < T_{\text{K}}$ ), the Kondo effect dominates and the ground state is non-magnetic. At intermediate values of  $JN$ , where both the interactions have comparable strength, non-Fermi liquid behaviour has been observed in several systems [3].

Since both the interactions depend on the product  $JN$ , their magnetic ground state will depend critically on the unit cell volume and number of electrons in the transition metal for  $\text{CeT}_2\text{X}_2$  systems. It has been observed that compounds with unit cell volume larger than  $\sim 170 \text{ \AA}^3$  order magnetically. One typical example is  $\text{CeRu}_2\text{Ge}_2$ , which has a unit cell volume

of 183 Å and orders ferromagnetically below 8 K [1, 4]. With the application of pressure it shows a magnetic to non-magnetic transition around 8 GPa [5]. Another method of varying the unit cell volume employed is the chemical pressure effect. The substitution of Si, which has smaller ionic radii than Ge, also shows results similar to external pressure studies [5, 6]. Fontes *et al* [7] has reported Fe substitution studies on the Ru site, which also show a magnetic to non-magnetic transition around  $x = 0.9$  for  $\text{Ce}(\text{Ru}_{1-x}\text{Fe}_x)_2\text{Ge}_2$ . However, the phase diagram presented by Fontes *et al* appears to be different compared to high-pressure and Si doping studies in  $\text{CeRu}_2\text{Ge}_2$ .

To understand the differences in the phase diagram of  $\text{CeRu}_2\text{Ge}_2$  we have substituted Co at the Ru site. Co is the nearest neighbour to Fe in the periodic table with comparable ionic radii. The series of compounds  $\text{CeRu}_{2-x}\text{Co}_x\text{Ge}_2$  ( $x = 0.0-2.0$ ) offers an interesting case to study, with variation in the competing strengths of RKKY interactions and Kondo effect interactions across the series. One end member of the series  $\text{CeRu}_2\text{Ge}_2$  ( $x = 0$ ), with unit cell volume 183 Å, has been reported to order ferromagnetically below 7.5 K [1, 4], whereas the other end member  $\text{CeCo}_2\text{Ge}_2$ , with unit cell volume 168 Å, is reported to be an intermediate valence compound with Kondo temperature 100 K [8]. It has been shown that  $\text{CeRu}_2\text{Ge}_2$  first orders antiferromagnetically around 8.5 K and then becomes ferromagnetic through a first order magnetic transition below 7.5 K [9, 10]. With the application of external pressure, initially the ferromagnetic transition is suppressed and the antiferromagnetic transition temperature increases. On further increasing the pressure the antiferromagnetic transition temperature decreases and the compound becomes non-magnetic around 8 GPa [5, 11–13]. Therefore it is interesting to see the effect of Co substitution on the Ru site as this is also expected to exert positive pressure with Co substitution. Besides the positive pressure effect, Co substitution at the Ru site may also modify  $N$  as the former has one additional d-electron compared to the latter.

In this paper we present our results on the crystal structure, electrical resistivity and magnetoresistance of the system  $\text{CeRu}_{2-x}\text{Co}_x\text{Ge}_2$ . With increasing  $x$  the unit cell volume decreases which drives the system from a magnetic to a non-magnetic regime.

## 2. Experimental details

The polycrystalline compounds  $\text{CeRu}_{2-x}\text{Co}_x\text{Ge}_2$  ( $x = 0, 0.5, 1.0, 1.5, 1.8$  and  $2.0$ ) were prepared by arc melting constituent elements of purity better than 99.9% (Ce and Ru) and 99.99% (Co and Ge). The compounds were melted several times for better homogeneity. As-prepared compounds were wrapped in Mo-foils and sealed in evacuated quartz ampoules in a vacuum of the order of  $10^{-5}$  Torr and kept for annealing at 800 °C for 5 days. For x-ray diffraction (XRD) measurements portions of the samples were cut and ground to make powder. The powder XRD measurements on all the samples were carried out using a rotating anode x-ray generator in the range  $10^\circ-80^\circ$ , with a step size of  $0.2^\circ$  and speed  $2^\circ \text{ min}^{-1}$ . The resistivity measurements were carried out using the standard four-probe method in the presence of He exchange gas and in the temperature range 1.5–300 K. Longitudinal magnetoresistance was measured at 5 K up to 8 T magnetic field for all the samples.

## 3. Results

The results of the powder XRD measurements on the compound  $\text{CeRu}_{2-x}\text{Co}_x\text{Ge}_2$  ( $x = 0.0-2.0$ ) are shown in figure 1. All the compounds order in the  $\text{ThCr}_2\text{Si}_2$  type crystal structure (figure 2) with space group  $I4/mmm$ . All the lines in the XRD pattern were identified with the above space group, indicating that all the compounds were single phase in nature.

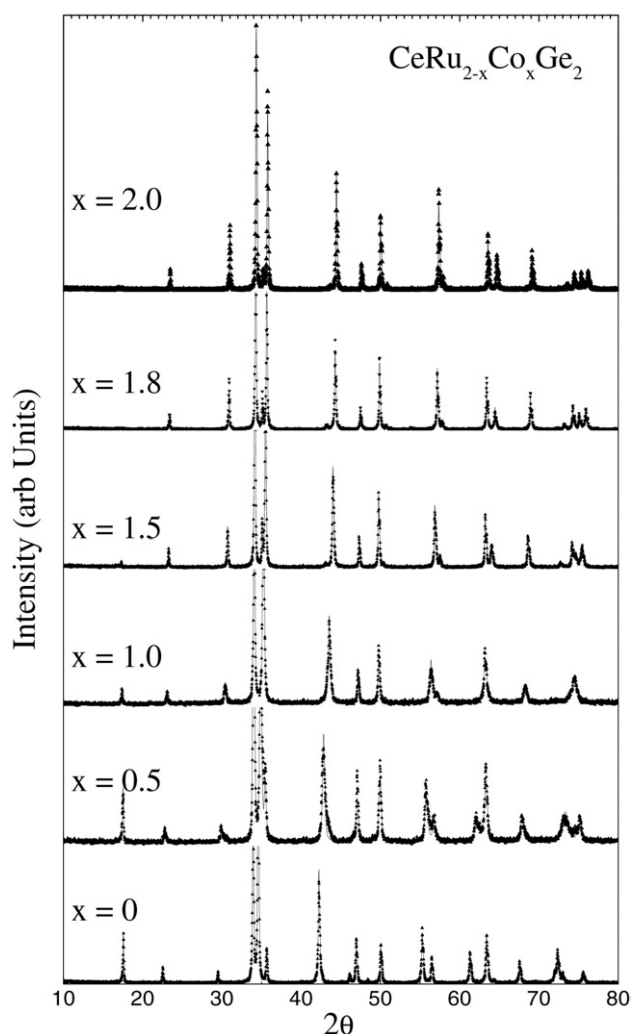


**Figure 1.** Powder x-ray diffraction pattern for the compounds  $\text{CeRu}_{2-x}\text{Co}_x\text{Ge}_2$  ( $x = 0.0-2.0$ ). The dots represent the observed data and line curves are the fitted pattern obtained from Rietveld refinement.

Structural refinement for all the compounds was carried out using DBWS software [14]. The lines in figure 1 show the fitted curve while the dots represent the observed data. For all the samples except  $x = 0.5$  the refined pattern shows excellent agreement with the observed pattern (see figure 1). This is reflected in the goodness of fit parameters summarized in table 1. The error bars on the refined structural parameters are thus also quite small. In case of  $x = 0.5$  composition, the refinement is not as good as for the other alloys, due to the asymmetry observed in some peaks at the higher angle side. The asymmetry in the peaks can be attributed to the strain in the unit cell as a result of doping. The unit cell parameter  $a$  and unit cell volume  $V$  show a linear decrease with increasing Co concentration ( $x$ ). This is expected, as Co ions have smaller ionic radii than Ru. However the  $z$ -coordinate of the Ge ions and the lattice cell parameter  $c$  increases non-monotonically with  $x$ . The variation of the unit cell parameters  $a$  and  $c$  and the volume are shown in figure 3.

The results of resistivity measurements, in the temperature region 1.5–300 K, are shown for all the compounds in figure 4. The resistivity values have been normalized to room temperature values of the respective compound. The sharp changes in the resistivity versus temperature

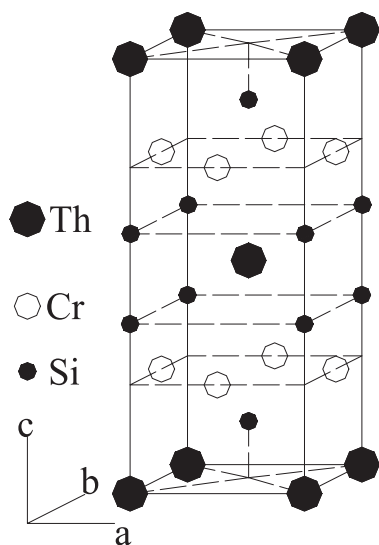


**Figure 2.** Schematic diagram of ThCr<sub>2</sub>Si<sub>2</sub> type unit cell.

**Table 1.** Structural parameters obtained from the Rietveld refinement of the powder x-ray diffraction data for the system CeRu<sub>2-x</sub>Co<sub>x</sub>Ge<sub>2</sub> ( $x = 0.0-2.0$ ).

$x$	0.0	0.5	1.0	1.5	1.8	2.0
$a$ (Å)	4.2684(1)	4.2210(4)	4.1543(3)	4.1060(2)	4.0815(1)	4.0674(1)
$c$ (Å)	10.0471(4)	10.1204(10)	10.1887(9)	10.2088(4)	10.1963(3)	10.1740(3)
$V$ (Å <sup>3</sup> )	183.05(1)	180.31(3)	175.84(2)	172.11(1)	169.86(1)	168.32(1)
$Z$	0.3679(3)	0.3706(4)	0.3707(3)	0.3702(2)	0.3701(2)	0.3690(2)
Ce-T (Å)	3.2960	3.2948	3.2867	3.2754	3.2653	3.2566
Ce-Ge (Å)	3.2971	3.2594	3.2194	3.1915	3.1755	3.1699
Ce-Ce (Å)	4.2684(1)	4.2210(4)	4.1543(3)	4.1060(2)	4.0815(1)	4.0674(1)
R-P	12.06	19.43	14.37	13.39	15.28	14.16
$R_{WP}$	18.02	25.14	18.46	19.16	20.50	19.25
$R_{expected}$	13.24	14.27	14.20	14.16	14.63	14.89
$S$	1.36	1.76	1.30	1.35	1.40	1.29

curve for the compounds  $x = 0, 0.5$  and  $1.0$ , which are highlighted in the inset of figure 4, indicate the onset of magnetic ordering. The ordering temperatures, taken as the maxima in the temperature derivatives of the resistivity, are found to be 7.5, 8.5 and 6.5 K respectively. A careful observation of the inset of figure 4 reveals many important features. The resistivity curve for  $x = 0$  starts decreasing rapidly below  $\sim 8.5$  K, while the derivative show a maximum around 7.5 K. This behaviour suggests two magnetic transitions in agreement with earlier reports [4, 9]. The first one around 8.5 K represents the paramagnetic (PM) to antiferromagnetic (AFM) transition and the other one around 7.5 K represents the antiferromagnetic (AFM) to ferromagnetic (FM) transition. The two transitions are clearly seen in the  $x = 0.5$  composition. In this case the AFM-FM transition shifts to lower temperatures (6 K) while the PM-AFM transition remains at 8.5 K. For  $x = 1.0$  there is only one magnetic transition around 6.5 K, which is a PM-AFM transition as verified from the magnetoresistance measurements discussed below. For all the three compositions discussed above, besides the sharp drop in resistivity below the magnetic ordering temperature there is an increase in resistivity with decreasing temperature just above the magnetic ordering temperature. This increase in resistivity with decreasing temperature becomes more prominent with increasing Co concentration. This

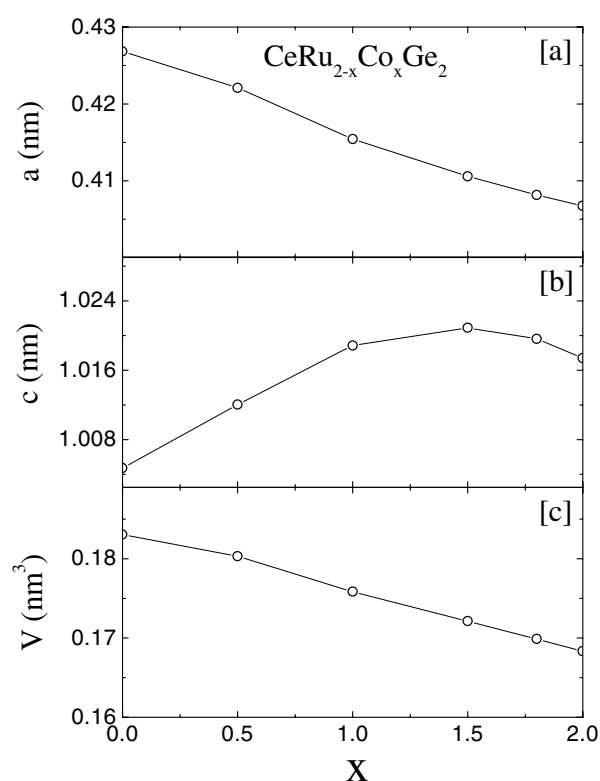


**Figure 3.** Variation of unit cell parameter (a)  $a$  in nm, (b)  $c$  in nm, and (c) unit cell volume  $V$  in  $\text{nm}^3$  as a function of Co ion concentration ( $x$ ) for  $\text{CeRu}_{2-x}\text{Co}_x\text{Ge}_2$ . The lines through the data points are guides to the eyes.

behaviour is arising due to the Kondo effect, which becomes more prominent with decreasing unit cell volume, i.e. increasing Co concentration. For other compositions  $x = 1.5, 1.8$  and  $2.0$ , magnetic ordering has not been observed in the entire temperature range studied, and the resistivity shows a broad maximum. In the case of the  $x = 2.0$  compound the broad maximum in the resistivity has been attributed to the valence fluctuating behaviour observed in this compound [8, 15].

In order to understand the nature of the magnetic transitions observed, magnetoresistance ( $\Delta\rho/\rho$ ) measurements at 5 K were performed, the results of which are shown in figure 5. These  $\Delta\rho/\rho$  results are in qualitative agreement with the magnetoresistance studies of  $\text{CeRu}_2\text{Ge}_2$  under external pressure by Kobayashi *et al* [13] and Süllo *et al* [16]. For  $x = 0$  and  $0.5$ ,  $\Delta\rho/\rho$  is negative, and its magnitude increases rapidly at low fields and tend to saturate at high field values. This shows that the transitions at 7.5 and 6 K observed in these compositions are ferromagnetic in nature. The  $\Delta\rho/\rho$  behaviour for these two compositions is similar to the magnetoresistance behaviour of  $\text{CeRu}_2\text{Ge}_2$  at 1.5 K under 5 Gpa pressure, as studied by Kobayashi *et al* [13]. For the compound with  $x = 1.0$  the magnetoresistance is small, positive and increases with increasing field up to 0.8 T, which is typical of an antiferromagnet. Beyond 0.8 T it decreases rapidly with further increase in magnetic field, which is a signature of a metamagnetic transition. For the composition  $x = 1.5$  the magnetoresistance is typical of paramagnets, showing negative  $H^2$ -like dependence. For  $x = 1.8$  and  $2.0$ , the magnetoresistance is negligible and slightly positive for the latter, which indicates the non-magnetic nature of these compounds. Our  $\Delta\rho/\rho$  results for  $x = 1.0, 1.5$  and  $1.8$  are similar to the  $\Delta\rho/\rho$  behaviour of  $\text{CeRu}_2\text{Ge}_2$  at 6 K under an external pressure of 5.8, 6.4 and 7.6 GPa

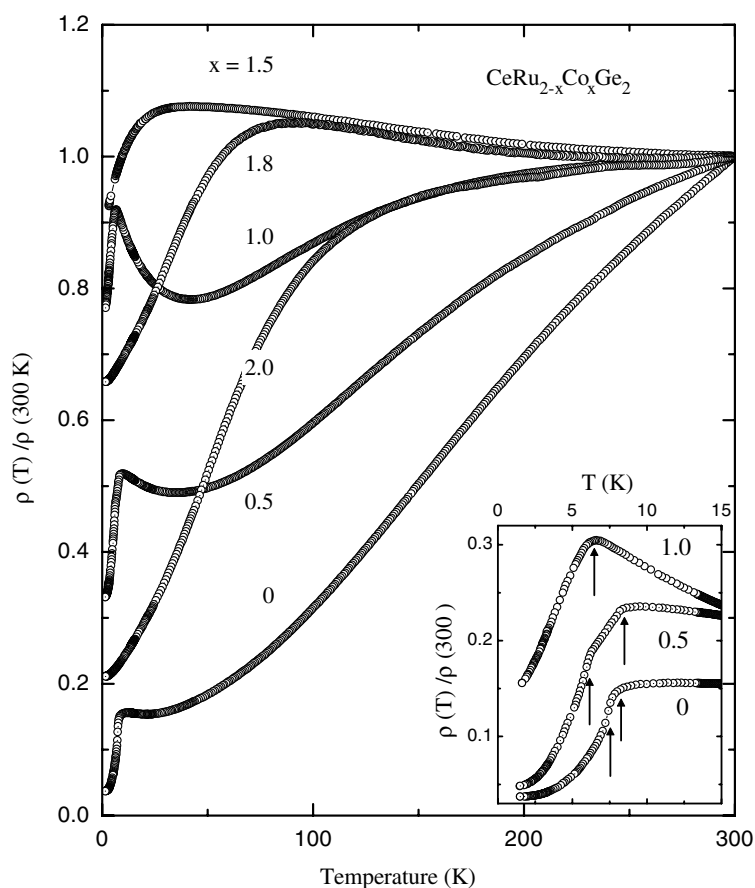


**Figure 4.** Temperature dependence of resistivity ( $\rho$ ) normalized to room temperature values for  $\text{CeRu}_{2-x}\text{Co}_x\text{Ge}_2$ . The inset shows the low temperature region for  $x = 0, 0.5, 1.0$  and the arrows indicate the magnetic transition temperature. The curves for  $x = 0.5$  and  $1.0$  are shifted in the inset for clarity.

respectively by Süllow *et al* [16]. The positive small magnetoresistance has been observed at 10 GPa for  $\text{CeRu}_2\text{Ge}_2$  by Kobayashi [13] *et al*, which is similar to our magnetoresistance behaviour for the  $x = 2.0$  composition.

#### 4. Discussion

The Co ion has smaller ionic radii compared to Ru radii, therefore with the substitution of Co in place of Ru, the unit cell volume is expected to decrease (figure 2(c)). The non-monotonic variation of the  $c$  or  $z$  parameter appears to be a result of chemical disorder in this system, which is inherent in substitutional alloys. This is further supported by the concentration dependence of the residual resistivity ratio (RRR) [ $\rho(300\text{ K})/\rho(1.5\text{ K})$ ] as shown in figure 6. It is well known that the residual resistivity ratio gives an indication of the disorder in the sample: the higher the ratio the less the disorder. In figure 6, RRR as a function of  $x$  shows a shallow minimum for intermediate compositions. A similar but opposite behaviour is seen for the  $z$  coordinate of the Ge ion.

With the substitution of Co at Ru ion sites the lattice volume decreases, therefore the exchange integral  $J$  between conduction electrons and Ce f-orbitals will increase with

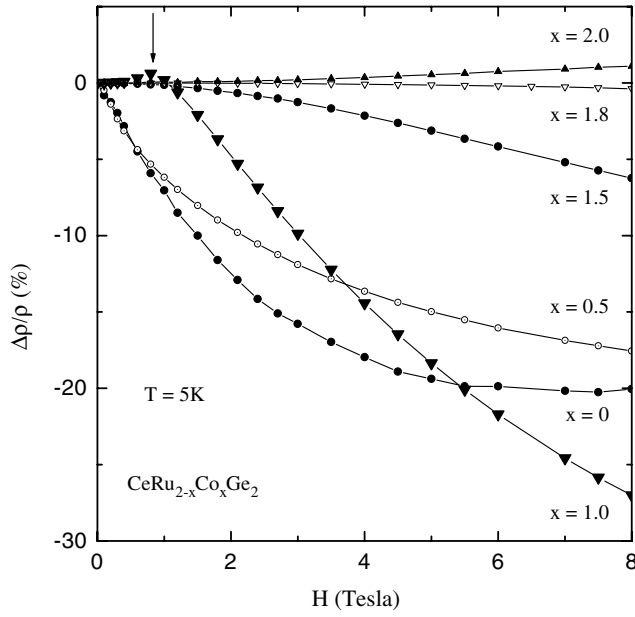


**Figure 5.** Magnetoresistance ( $\Delta\rho/\rho$ , where  $\Delta\rho = \rho(H) - \rho(0)$ ), as a function of magnetic field ( $H$ ) for  $\text{CeRu}_{2-x}\text{Co}_x\text{Ge}_2$ . The arrow indicates the critical magnetic field for the metamagnetic transitions for the composition  $x = 1.0$ . The lines through the data points are guides to the eye.

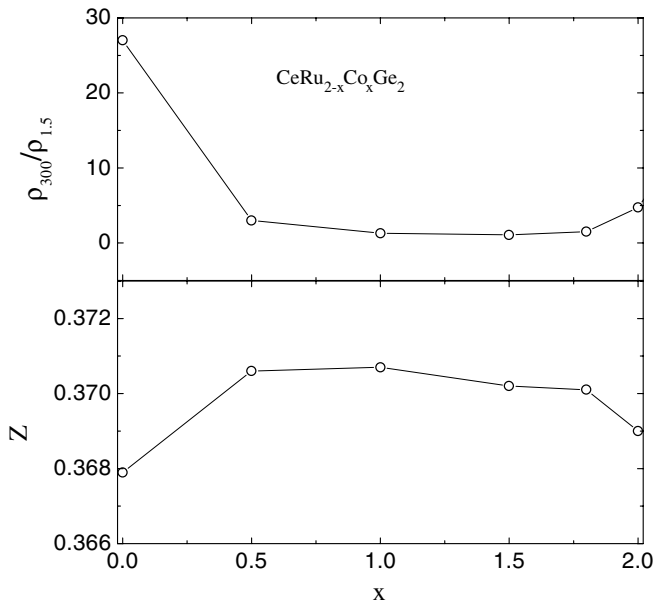


**Figure 6.** (a) Residual resistivity ratio  $\{\rho(300\text{ K})/\rho(1.5\text{ K})\}$  and (b)  $z$  coordinate of Ge ion in the unit cell as a function of Co ion concentration. The lines through the data points are guides to the eyes.

increasing Co concentration. This increase in  $J$  first increases the magnetic ordering temperature as the strength of RKKY interaction  $T_{\text{RKKY}}$  has  $(JN)^2$  dependence whereas the Kondo interaction strength  $T_K$  has  $\exp(-1/JN)$  dependence. With further increase in  $J$ , both the Kondo effect and RKKY interactions will have comparable strength for certain values of  $J$ ; therefore, the rise in magnetic ordering temperature with increasing  $J$  tends to saturate. This is the case for  $x = 0$  and  $0.5$  compositions, where both the interactions are of comparable strength, thereby showing a PM to AFM transition at the same temperature (8.5 K) though the lattice volume has been changed by nearly 1.5%. With further decrease in



lattice volume (increase in  $J$ ) the Kondo effect starts dominating, and therefore the magnetic ordering temperature starts decreasing ( $x = 0.5$ – $1.0$ ). The dominance of the Kondo effect is also evident from the observed resistivity rise above the magnetic ordering temperature in these compositions. With increasing  $x$  the resistivity rise is more pronounced. Finally, the magnetic ordering vanishes, and no magnetic ordering has been observed for  $x > 1.0$ . The compounds with  $x = 1.5$ ,  $1.8$  and  $2.0$  are thus non-magnetic and show broad shoulders around 30, 60 and 100 K, below which there is a large drop in resistivity. As mentioned earlier, the compound  $\text{CeCo}_2\text{Ge}_2$  is reported to be an intermediate valence compound with Kondo temperature around 100 K [8, 15]. Therefore the broad shoulders in these compounds may be associated with intermediate valence behaviour. That the resistivity decrease in these compounds ( $x = 1.5$ – $2.0$ ) is not related to magnetic ordering is further confirmed by the magnetoresistance measurements at 5 K. The compounds with  $x \leq 1.0$  give a clear signature of a magnetically ordered state. It is ferromagnetic-like for  $x = 0$  and  $0.5$ , and in the case of  $x = 1.0$  it shows a metamagnetic transition around 0.8 T, whereas the composition  $x = 1.5$  shows negative  $H^2$ -like variation of magnetoresistance which is typical of a paramagnet. The compositions  $x = 1.8$  and  $2.0$  show negligible magnetoresistance, typical of non-magnetic metals.

Based on the above results a tentative magnetic phase diagram with normalized unit cell volume ( $V/V_0$ , where  $V_0$  is the unit cell volume of  $\text{CeRu}_2\text{Ge}_2$ ) and Co concentration ( $x$ ) for the system  $\text{CeRu}_{2-x}\text{Co}_x\text{Ge}_2$  has been drawn in figure 7(a). From this phase diagram the quantum critical point is expected to occur for compositions between  $x = 1.0$  and  $1.5$ , i.e. for a unit cell volume between 175 and 172 Å. The trend of our phase diagram appears to be similar to the phase diagram of  $\text{CeRu}_2\text{Ge}_2$  under external pressure studied by Wilhelm *et al* [5] (shown by dotted lines in figure 7(a)). In both cases the AFM–FM transition temperature decreases rapidly, and the PM–AFM transition temperature initially remains more or less constant and then starts decreasing rapidly to zero. However, there are subtle differences between the two phase diagrams. In the case of Wilhelm *et al*, the AFM–FM transition temperature has been decreased from 7.5 to less than 4 K for  $V/V_0 = 1$ – $0.985$  and the PM–AFM transition temperature has been increased from 8.5 to 10 K. In our case the PM–AFM transition temperature is almost constant whereas the AFM–FM transition temperature is decreased to 6 K only for the same volume change. With further reduction in volume or increase in Co doping the PM–AFM transition temperature decreases to 6.5 K, whereas in case of high-pressure studies it is around 9 K for a corresponding volume change.

The difference between the two studies can be understood from the expression for the exchange coupling  $J$ , which can be written as [17]

$$J \propto V_{cf}^2 / (E_F - E_f),$$

where  $E_F$  is the Fermi energy,  $E_f$  is f-level energy and  $V_{cf}$  is the hybridization matrix element, which can be written as [18]

$$V_{ll'm} = \frac{\eta_{ll'm} \hbar^2}{m_e} \left[ \frac{(r_l^{2l-1} r_{l'}^{2l'-1})^{1/2}}{d^{l+l'+1}} \right]$$

with interatomic distance  $d$ , the angular momentum of the orbitals  $l$  and  $l'$ , the atomic shell radius  $r$  and the symmetry of the bond  $m$ . From this relation it is evident that the exchange coupling depends on the interatomic distance between the ions. A glance at the various bond distances in table 1 shows that the variation of Ce–Ru/Co (Ce–T) bond distance follows a trend similar to the concentration dependence of the magnetic transition temperature. The volume dependence of the Ce–T bond distance is plotted in figure 7(b). It shows that for a relative volume change from 1.0 to 0.985 the Ce–T distance is decreased by only 0.04%. However,

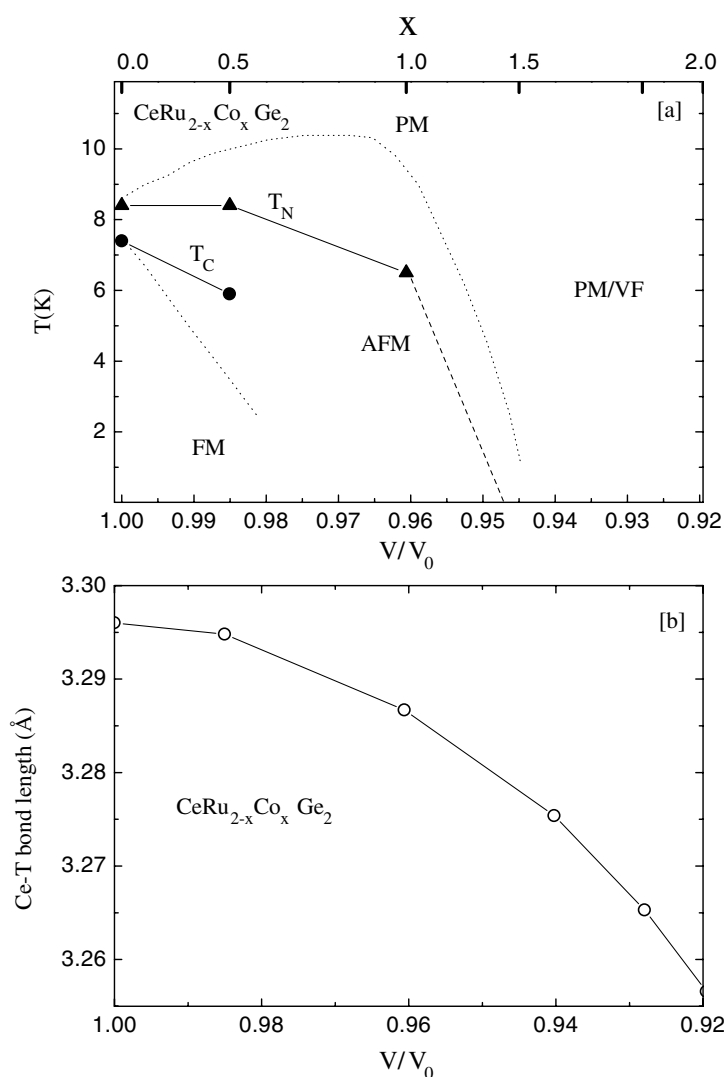


**Figure 7.** (a) Proposed magnetic phase diagram for  $\text{CeRu}_{2-x}\text{Co}_x\text{Ge}_2$  as a function of  $V/V_0$ , i.e. unit cell volume normalized to  $x = 0.0$  composition (bottom axis) and Co ion concentration ( $x$ ) (top axis). The lines between the data points are guides to the eyes. The dotted lines show the magnetic phase diagram of  $\text{CeRu}_2\text{Ge}_2$  with  $V/V_0$  taken from Wilhelm *et al* [5]. (b) Variation of Ce-T bond length with  $V/V_0$  for  $\text{CeRu}_{2-x}\text{Co}_x\text{Ge}_2$ .

with further decrease in lattice volume it starts decreasing rapidly. It is worth noting here that the volumes and correspondingly the bond distances are calculated in an indirect manner in the high-pressure study by Wilhelm *et al* [5], whereas, in our case we deduced the unit cell volume and bond distances directly from the x-ray diffraction data, thereby giving unambiguous results. This correlation between Ce-T bond distance and magnetic transition temperature shows that f-d hybridization is the main effect in determining the exchange coupling  $J$  and therefore the magnetic properties of  $\text{CeRu}_{2-x}\text{Co}_x\text{Ge}_2$  system.

The substitution of Co in place of Ru may also change  $N$  (the density of state at the Fermi level), as Co has one additional d-electron compared to the Ru ion. In the light of the present

investigation the effect of varying  $N$  appears to be small compared to the volume effect, as has been indicated by the correlation between the Ce–T bond distance and the magnetic transition temperature mentioned above. To explore the small effect of varying  $N$  more experiments like XPS, heat capacity and band structure calculation will be required.

Fontes *et al* [7] have also drawn a tentative phase diagram for the system  $\text{CeRu}_{2-x}\text{Fe}_x\text{Ge}_2$  with Fe doping at the Ru site. This phase diagram with Fe doping appears to be entirely different when compared to our Co doped system as well as the high-pressure studies of Wilhelm *et al* [5]. Fontes *et al* have not observed any AFM to FM transition for any Fe concentration. This is surprising, considering the fact that Fe and Co are near neighbours in the periodic table and have similar ionic radii. This difference may be arising due to the increase in Ce–Ru/Fe bond length with decreasing unit cell volume (i.e. with increasing Fe concentration), whereas in our case and in the high-pressure studies it decreases with decreasing unit cell volume.

## 5. Conclusions

The structural and electrical transport studies of  $\text{CeRu}_{2-x}\text{Co}_x\text{Ge}_2$  have been carried out. These studies showed that the system is driven from a magnetic to a non-magnetic ground state as an effect of Co doping on the Ru site. The transition of the ground state is due to volume effects occurring due to the Co doping. The nature of magnetic transitions was confirmed by magnetoresistance measurements. Magnetoresistance studies also showed that the system undergoes a metamagnetic transition for  $x = 1.0$  around 0.8 T magnetic field. The magnetic phase diagram for the system  $\text{CeRu}_{2-x}\text{Co}_x\text{Ge}_2$  is proposed and from this phase diagram the quantum critical point is expected for a composition between  $x = 1.0$  and 1.5, i.e. for a unit cell volume between 175 and 172 Å<sup>3</sup>. These studies also showed that the Ce–Ru/Co bond distance plays a critical role in driving the system from an RKKY dominated regime to a Kondo regime.

## Acknowledgment

The authors would like to thank Dr N P Lalla, UDC Indore for providing XRD measurement facility.

## References

- [1] Szytula A 1991 *Handbook of Magnetic Materials* vol 6, ed K H J Buschow (Amsterdam: Elsevier Science) p 85
- [2] Doniach S 1977 *Physica B* **91** 231
- [3] Stewart G R 2001 *Rev. Mod. Phys.* **73** 797
- [4] Bohm A, Caspary R, Habel U, Pawlak L, Zuber A, Steglich F and Loidl A 1988 *J. Magn. Magn. Mater.* **76/77** 150
- [5] Wilhelm H, Alami-Yadri K, Revaz B and Jaccard D 1999 *Phys. Rev. B* **59** 3651
- [6] Hean P, Mallmann F, Besnus M J, Kappler J P, Bourdarot F, Burllet P and Fukuhara T 1996 *J. Phys. Soc. Japan* **65** (Suppl.B) 16
- [7] Fontes M B, Continentino M A, Bud'ko S L, El-Massalami M, Sampaio L C, Guimaraes A P, Baggio-Saitovitch E, Hundley M F and Lacerda A 1996 *Phys. Rev. B* **53** 11678
- [8] Fujii H, Ueda E, Uwatoko Y and Shigeoka T 1988 *J. Magn. Magn. Mater.* **76/77** 179
- [9] Thompson J D *et al* 1994 *Physica B* **199/200** 589
- [10] Wilhelm H and Jaccard D 1998 *Solid State Commun.* **106** 239
- [11] Bouquet F, Wang Y, Wilhelm H, Jaccard D and Junod A 2000 *Solid State Commun.* **113** 367
- [12] Wilhelm H and Jaccard D 1999 *Physica B* **259–261** 79
- [13] Kobayashi T C, Miyazu T, Shimizu K, Amaya K, Kitaoka Y, Onuki Y, Shirase M and Takabatake T 1998 *Phys. Rev. B* **57** 5025
- [14] Wiles D B and Yong R A 1981 *J. Appl. Crystallogr.* **14** 149
- [15] Moon E D, Hong S O, Kim D L, Ri H C and Kwon Y S 2003 *Physica B* **329–333** 516
- [16] Süllow S, Aronson M C, Rainford B D and Haen P 1999 *Physica B* **259–261** 54
- [17] Schrieffer J R and Wolff P A 1966 *Phys. Rev. B* **149** 491
- [18] Harrison W A 1983 *Phys. Rev. B* **28** 550